

## Some Peculiarities in Deformation and Fracture Behaviour of Austempered Ductile Cast Iron

Jan KOHOUT<sup>1\*</sup>, Stanislav VĚCHET<sup>2</sup>

<sup>1</sup>Department of Physics, Military Technology Faculty, University of Defence, Kounicova St 65, CZ-612 00 Brno, Czech Republic

<sup>2</sup>Faculty of Mechanical Engineering, Brno University of Technology, Technická St 2, CZ-616 69 Brno, Czech Republic

Received 02 June 2005; accepted 07 July 2005

Tensile tests and fracture toughness tests of an unalloyed austempered ductile cast iron (ADI) with the matrix created by upper bainite and containing 30 to 35 % of retained austenite were performed in a temperature range  $-196^{\circ}\text{C}$  to  $+200^{\circ}\text{C}$  to study its mechanical behaviour. The temperature dependence of true fracture stress, elongation to fracture, and reduction of area is separated into three regions with different fracture behaviour. Unmonotonous temperature dependence of yield points defined by plastic strain of 0.05 to 2 % is evidence of the stress induced phase transformation of retained austenite into martensite before these values of plastic strain are reached. The transformation of retained austenite is also substantiated with an increase of hardness and in several cases the decrease of retained austenite content was directly determined with X-ray quantitative phase analysis. Also higher values of dynamic than of static fracture toughness are evidence of unusual behaviour of ADI due to retained austenite presence in ADI structure.

**Keywords:** ADI, tensile tests, yield stress, fracture toughness, retained austenite.

### 1. INTRODUCTION

Owing to its excellent mechanical as well as technological properties, *austempered* (i.e. isothermally heat treated) *ductile* (or now more often called nodular) cast *iron* (ADI) belongs among prospective structural materials. Recently it is applied to castings for dynamically loaded components, e.g. gear and traversing wheels, crankshafts of motor-cars, vans and trucks, swivel pins, rail brakes, pressure pipes in oil industry etc. [1, 2]. Considerable part of ADI production is applied in military industry, e.g. in 1995 about 3 % of total ADI production in U.S.A. was used for military reasons [2].

ADI castings are preferably applied in these cases [3]:

1. Most usual case consists in the substitution of a detail made of steel (forged piece, workpiece or weldment) when the design remains the same as the design of the original detail or only slight changes of it are made.
2. Not so often the casting made of nodular cast iron with lower level of strength properties (usually with pearlitic matrix) is substituted with ADI casting to increase its loading capacity and/or its service life.
3. In the case when a new detail is designed specially for ADI application (above all when a complex of heat treated details is substituted with only one ADI casting, e.g. steering swivel pin in motor-cars), the highest savings are obtained.

Microstructure and mechanical properties of ADI can be substantially influenced by the condition of heat treatment, above all by the temperature of isothermal transformation. According to this temperature various bainitic matrices are obtained, containing various content of retained austenite (RA). For transformation temperature about  $350^{\circ}\text{C}$  transition bainite is obtained. Higher transformation temperatures lead to upper bainite which is

very tough due to higher content of RA but also has good strength properties. On the contrary, lower transformation temperatures lead to lower bainite with lower content of RA. Its advantages consist in extremely high strength and a satisfactory level of deformability and toughness.

Phase transformation of austenite into martensite caused by mechanical loading is very well known also for RA in austempered ductile cast irons [3]. Usually this phenomenon was explained by the TRIP effect. But only Tamura [4] described in fine detail also stress induced transformation of austenite by simultaneously acting mechanical loading and temperature decrease.

### 2. EXPERIMENTAL

The chemical composition of studied nodular cast iron was 3.46 wt % C, 2.11 % Si, 0.24 % Mn, 0.054 % P, 0.021 % S, and 0.058 % Mg. Its thermal treatment consisted of austenitization at  $900^{\circ}\text{C}$  during 60 minutes and isothermal quenching at  $400^{\circ}\text{C}$  taking 100 minutes in salt bath with water bath in the end. The grains of graphite were nearly perfectly globular with a size of 30 to 60  $\mu\text{m}$ . The matrix was created by upper bainite containing 30 to 35 vol. % of RA. Martensite whose existence in microstructure is very probable due to water bath in the end of thermal treatment was not shown by classical metallographical technique.

For tensile tests the samples of 6 mm in diameter and of 30 mm in nominal length were used, ended with threaded heads and loaded at a strain rate of  $5 \cdot 10^{-4} \text{ s}^{-1}$ . Static fracture toughness was determined using standard precracked samples of 12.5 mm in thickness for three-point bend at a stress intensity parameter rate of about  $0.5 \text{ MPa m}^{1/2} \text{ s}^{-1}$ . Samples  $10 \times 10 \times 55 \text{ mm}$  (Charpy V-notch impact specimens with fatigue crack in the notch) for the measurement of dynamic fracture toughness were chosen to obtain bainitic structure through all cross section. They were loaded using a swinging pendulum in bending

\*Corresponding author. Tel.: +420-973443283; fax.: +420-973442888. E-mail address: jan.kohout@unob.cz (J. Kohout)

at stress intensity parameter rate of about  $10^5 \text{ MPa m}^{1/2} \text{ s}^{-1}$ . Most of these mechanical tests were performed at temperatures between the temperature of liquid nitrogen and  $200^\circ\text{C}$ . The temperature was controlled and measured with accuracy better than  $1^\circ\text{C}$ .

The content of RA was determined by X-ray quantitative method. The Brinell hardness test with a ball of 2.5 mm in diameter and a loading of 187.5 kg was chosen to determine the average hardness on sufficiently large area of very heterogeneous structural mixture. Both RA content and the Brinell hardness were determined simultaneously in deformed and non-deformed parts of tensile test bars, i.e. in cylindrical parts and in threaded heads.

### 3. RESULTS

#### 3.1. Fracture behaviour

Temperature dependence of true fracture stress  $\sigma_{FR}$  (a quotient of fracture force and fracture cross section), reduction of area  $Z$ , and elongation to fracture  $A_5$  (so-called *short* samples were tested whose ratio of measured length and diameter is 5) is drawn in Fig. 1. Also ultimate tensile stress (*UTS*) is added but only fitted curve without experimental points. As the fracture appears at the highest loading force, a simple relation  $UTS = \sigma_{FR} (1 - Z)$  is valid among mentioned mechanical characteristics.

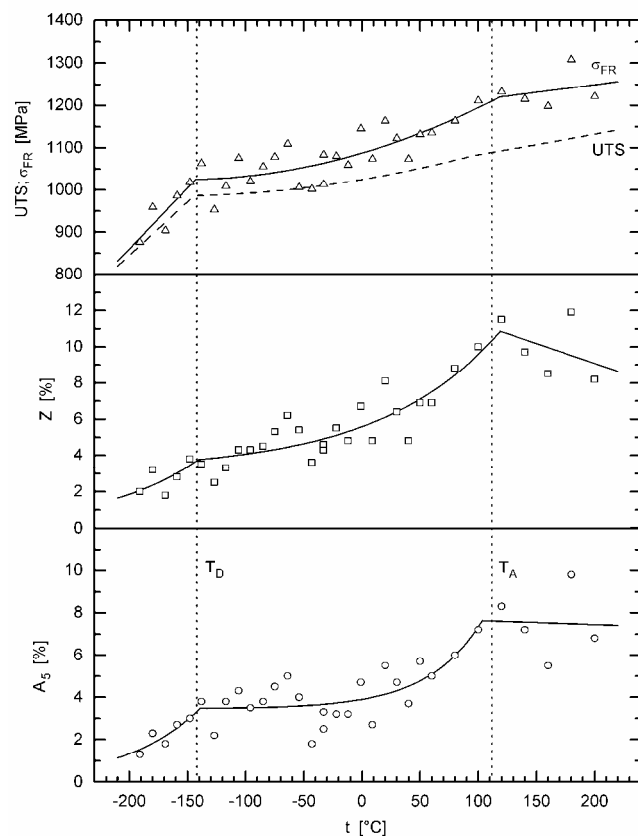


**Fig. 1.** Temperature dependence of true fracture stress  $\sigma_{FR}$ , reduction of area  $Z$ , and elongation to fracture  $A_5$  determines transition temperatures  $T_D$  and  $T_A$  dividing the temperature range of tests into three subregions. Also temperature dependence of ultimate tensile strength  $UTS$  is added

Fig. 1 shows that the temperature range of tests can be divided into three subregions and in each of them a different dominant mechanism of deformation and fracture can be expected. Therefore, each of regression functions was created by the combination of three simple functions: by linear, quadratic, and linear functions for true fracture stress and by two exponential and one linear function for deformation characteristics. In this manner two temperatures  $T_D$  and  $T_A$  determining the temperature subregions can be calculated using regression analysis. Thus for the temperature  $T_D$  the values  $(-143 \pm 16)^\circ\text{C}$ ,  $(-140 \pm 25)^\circ\text{C}$ , and  $(-141 \pm 36)^\circ\text{C}$  were determined by the fit of  $\sigma_{FR}$ ,  $Z$ , and  $A_5$ , respectively. Their weighted mean is  $T_D = (-142 \pm 13)^\circ\text{C}$ . Similarly, for the temperature  $T_A$  the values  $(118 \pm 46)^\circ\text{C}$ ,  $(103 \pm 16)^\circ\text{C}$ , and  $(119 \pm 18)^\circ\text{C}$  with weighted mean  $T_A = (111 \pm 12)^\circ\text{C}$  were determined.

In Fig. 1 a very high scatter of experimental results can be seen. Relatively high scatter is characteristic for the here represented mechanical properties characterizing the fracture as a final stage of the whole deformation process and higher scatter can be expected for ADI as a cast material. On the other hand, the scatter of Young's modulus characterizing elastic strain in the only beginning of loading is also extremely high for ADI (see Fig. 2) although it is quite low for most other structural materials. This is evidence of very high degree of heterogeneity in ADI microstructure.

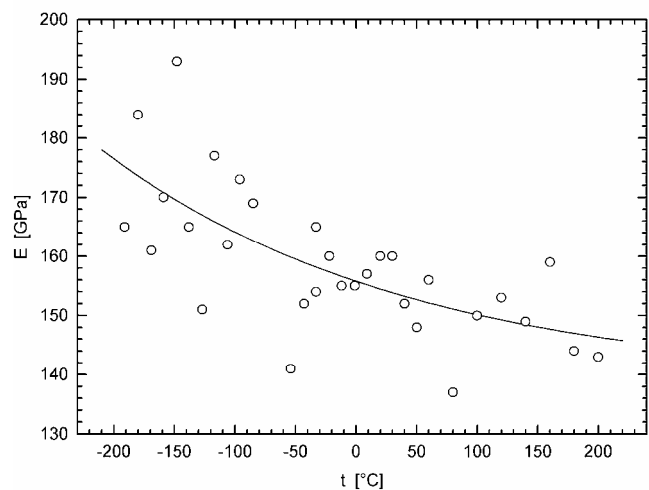


**Fig. 2.** Large scatter of temperature dependence of Young's modulus demonstrating high degree of ADI heterogeneity

The manifestation of the heterogeneity of tested material can be principally limited by increasing diameter of tested samples but with respect to extremely high tensile strength, such samples are of the capacity of available testing device.

A microfractographical study of fracture surfaces shows quasi-cleavage failure at temperature of  $-191^\circ\text{C}$  and ductile dimple failure at a temperature of  $200^\circ\text{C}$ . The mixture of both these types of failure was observed on the fractures of samples tested at room temperature and ductile dimple failure was situated around graphite nodules and among quasi-cleavage facets [5]. Due to high degree of heterogeneity in structure, very different places can be found on fracture surface. Therefore the classification and

representation of fracture surface as a whole is quite difficult.

### 3.2. Deformation and transformation of RA

The high content of RA together with decreasing temperature and tensile loading leads to the transformation of the austenite. Evidence of the transformation is given in the upper part of Fig. 3 by temperature dependence of hardness increase and RA content decrease fitted with Gaussian curves. The maximum increase of hardness is  $\Delta BHN = (56 \pm 6)$ . (Brinell hardness number, corresponding to  $1 \text{ kp/mm}^2$ ) and the maximum decrease of retained austenite content  $-\Delta RA$  is  $(15 \pm 2)$  vol. %. These maxima are reached at nearly identical temperatures,  $(-106 \pm 4)^\circ\text{C}$  and  $(-108 \pm 7)^\circ\text{C}$ , respectively.

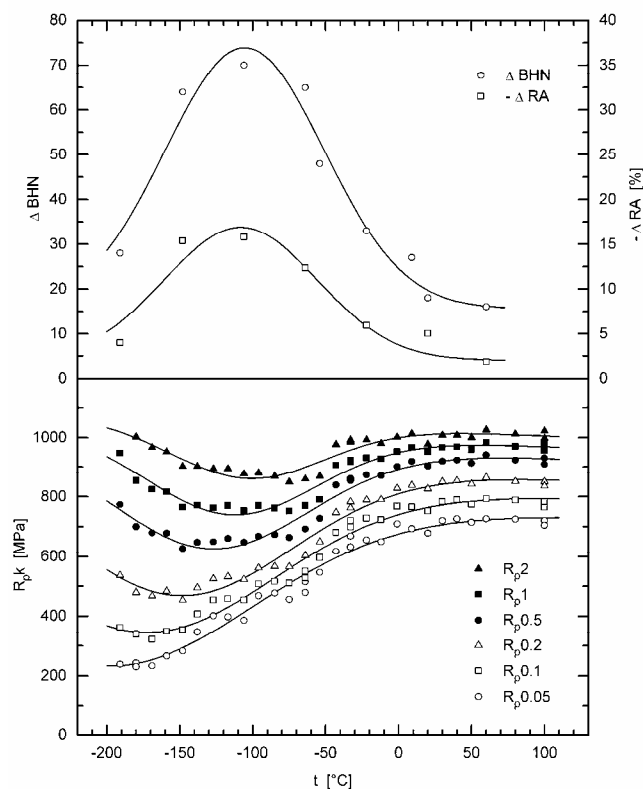


**Fig. 3.** Temperature dependence of hardness increase  $\Delta BHN$ , retained austenite content decrease  $-\Delta RA$ , and conventional yield points  $R_{p,k}$  for  $k$  0.05 to 2 %

Other evidence of the transformation of RA is given by unmonotonous temperature dependence of yield points defined by plastic strain of 0.05 to 2 % which is plotted in lower part of Fig. 3. For its fit the combination of exponential and Gaussian curves (i.e. functions of  $\exp(-x)$  and  $\exp(-x^2)$  type) was used. The positions of  $\Delta BHN$  and  $-\Delta RA$  extremes correspond to the minimum of yield point  $R_{p,1.2}$  (the value of  $k = 1.2$  was determined by interpolation, see Fig. 4).

Rather high scatter of the values of yield points  $R_{p,k}$  is the consequence of high scatter of Young's modulus (see Fig. 2) which is used for yield point determination for materials without sharp yield stress. Besides, the samples were made from two cast blocks with rather different properties. The samples made from one of them were tested below a temperature of  $-50^\circ\text{C}$  and the samples

made from the other were tested above this temperature. The difference in the samples can be seen in Fig. 3 (on temperature dependence of  $R_{p,k}$ ) as a certain discontinuity at a temperature of about  $50^\circ\text{C}$ . Both these facts mean that only changes in hardness and RA content (i.e. their differences) lead to reasonable results and conclusions. The absolute values of both quantities in deformed and non-deformed parts of samples are unfortunately too dispersed for any convincing presentation.

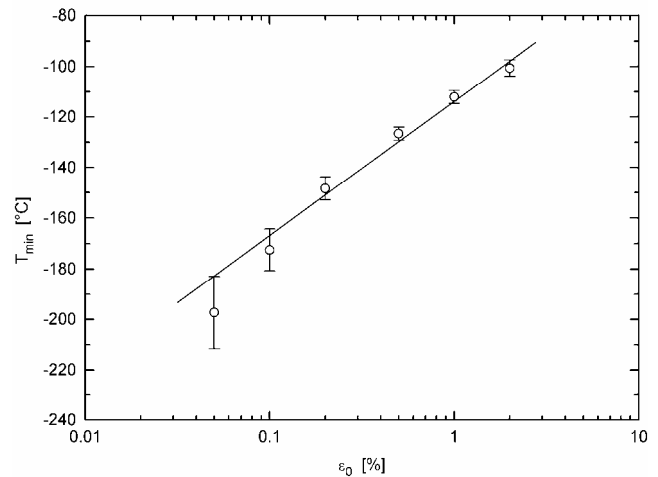


**Fig. 4.** Dependence of the position of yield points  $R_{p,k}$  minima on the defining plastic strain  $\varepsilon_0 = k$

The temperatures at which the minima of  $R_{p,k}$  lie are drawn in dependence on defining plastic strain  $\varepsilon_0$  in Fig. 4. The lower the defining strain, the lower the temperature of minimum stress  $T_{min}$  and the lower accuracy of its determination. It seems that  $T_{min}$  is approximately a linear function of the logarithm of  $\varepsilon_0$ .

Very interesting results were obtained by the determination of RA content along the sample after tensile test at a temperature of  $-117^\circ\text{C}$ , see Fig. 5. The results determined in the cylindrical part of the sample are fitted with the curve of  $(1 + x^2)^{-1}$  type, usually called the Cauchy (or the Lorentz) curve. While before the test the content of RA is nearly the same in the whole sample (about 35 % in the cylindrical part and about 32 % in the head due to its higher diameter), after the tensile test these values are saved only in non-deformed heads. The basic value of RA content of 24 % in deformed cylindrical part of tested sample (see extrapolated value in the right side of Fig. 5) decreases in the toe (the place of transition between cylindrical part of sample and threaded head) due to notch effect to a value of 21 % and in the most deformed spot to the minimum value of 17 %. But due to large hardening, this spot is not the place of final fracture which appears 5 mm farther. The content of RA near the fracture is (rather unexpectedly) only slightly lower (23 %) than the basic value. Here the fact must be added that each of these values of RA content was determined with an uncertainty of a few per cent.

### 3.3. Fracture toughness

The results of fracture toughness tests (static and dynamic) in dependence on temperature are presented in Fig. 6. While the values of static fracture toughness  $K_{IC}$  are

usually higher than the values of dynamic fracture toughness  $K_{I,d}$ , for ADI this relation is opposite. Some part of the difference can consist in different methodology of the determination of the force used for fracture toughness calculations: at static loading the force at first jump of crack (readable at loading diagram and well audible during ADI tests) was considered while at dynamic loading the maximum force was taken as a rule, having no other advisable possibility. But this fact is not sufficient for full explanation of higher values of dynamic fracture toughness.

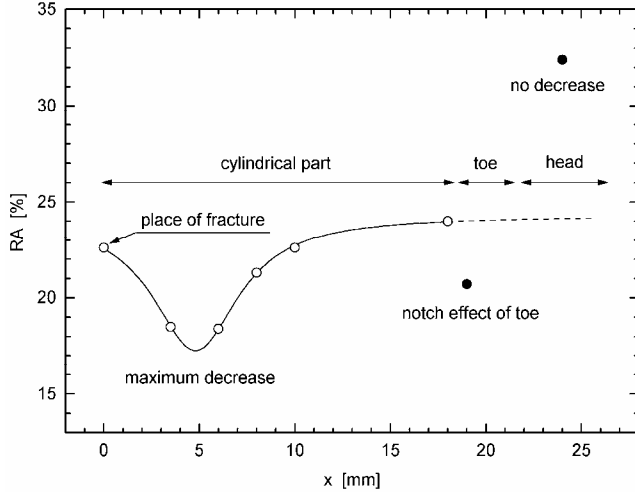


**Fig. 5.** Content of retained austenite along the sample tested at  $-117^{\circ}\text{C}$ , starting in fracture where  $x = 0$ . Cylindrical part, toe and head of sample are distinguished

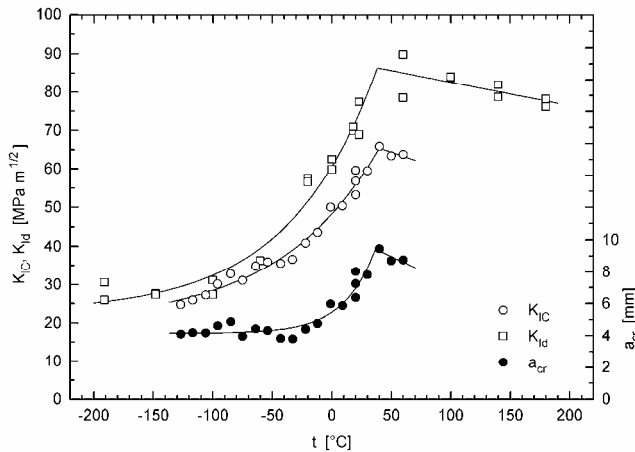


**Fig. 6.** Temperature dependence of static and dynamic fracture toughness ( $K_{IC}$  and  $K_{I,d}$ , respectively), and critical crack dimension  $a_{cr}$

Using relation:

$$a_{cr} = \frac{\pi}{2} \left( \frac{K_{IC}}{R_p 0.2} \right)^2, \quad (1)$$

critical crack dimension  $a_{cr}$  characterizing the resistance of the material against the effect of internal defects was calculated and its temperature dependence is also drawn in Fig. 6. Usually the values of critical crack dimension decrease very substantially with decreasing temperature. For the studied ADI nearly constant value of 4 mm is reached for wide range of negative centigrade

temperatures. This is the consequence of the fact that in this temperature range not only the values of fracture toughness but also the values of yield point decrease with decreasing temperature.

#### 4. DISCUSSION OF RESULTS

Unmonotonous temperature dependence of yield points defined by certain plastic strain is not a peculiarity only of upper bainite [5]. Besides upper bainite also transition bainite and lower bainite demonstrate similar temperature dependence of yield point  $R_p 0.2$  defined by plastic strain of 0.2 % (see Fig. 7) but the decrease of the yield point in the range of negative Celsius temperatures is substantially smaller because the content of RA in transition and lower bainite is lower (27 to 29 vol. % in transition bainite and 12 to 15 vol. % in lower bainite) and, consequently, also the decrease of RA content is lower.

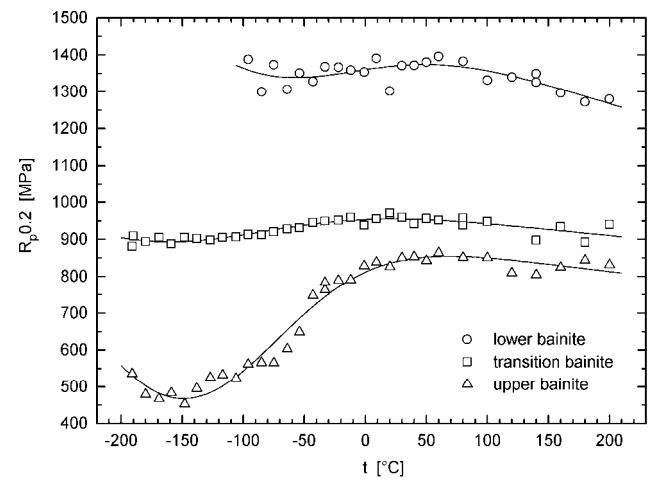


**Fig. 7.** Temperature dependence of proof stress  $R_p 0.2$  for matrices of lower, transition, and upper bainite

A special problem consists in the determination of RA content in ADI. The uncertainty of X-ray quantitative phase analysis alone is a few per cent. From this point of view the curve in Fig. 5 going exactly through all experimental points is not representative. But just this figure shows the variability of RA content along the cylindrical part of tested sample. The uncertainty of the analysis together with the variability depending on the choice of analyzed place is the reason why the scatter of RA content decrease in Fig. 3 is relatively high.

The matrix of studied ADI is created by very complicated mixture of upper bainite with high resistance to deformation and by retained austenite with extreme ability to be deformed even at very low temperature, which is the consequence of its FCC lattice. Also extremely strong and brittle martensite can be present in the structure. Besides its creation during thermal heating (which was finished by cooling in water bath), other reasons of its rise are possible: the effect of low temperature during temperature stabilization before the execution of the test at low temperatures, the effect of tensile loading during the test, and a common effect of low temperatures and tensile loading during the test [3 – 6]. The roles of decreased temperatures alone and of decreased temperatures together with the deformation during tensile tests on RA content are

compared in Fig. 8 for another melt of ADI with upper bainite matrix studied previously [3].

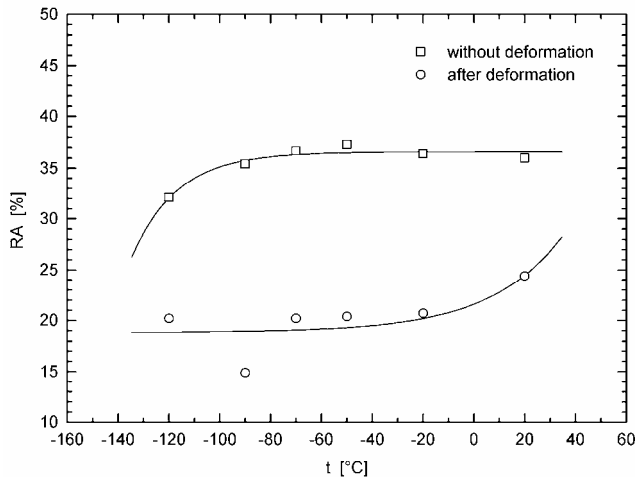


**Fig. 8.** Influence of temperature and deformation to fracture on RA content in tensile test bars (ADI with upper bainite matrix [3])

The transformation of retained austenite into martensite due to tensile loading is the consequence of greater specific volume of martensite than of austenite. But besides the main dimensional increase in the direction of loading force, also a dimensional increase appears in transversal directions. While usually reduction of area  $Z$  is substantially higher than elongation to fracture  $A_5$ , in the case of ADI both the quantities are very close (see Fig. 1). If the production of nodular cast iron is very successful (in the case of a melt with ideally globular graphite nodules and very low content of casting defects), the decrease of RA content can be over 20 %. In this case reduction of area can be considerably lower than elongation to fracture at room temperature and even negative values of reduction of area can be reached at low temperatures [6].

Unusual temperature dependence of yield stresses  $R_p k$  is one of consequences of austenite transformation. Missing sharp yield stress means to use conventional yield point defined by given plastic strain  $\varepsilon_0 = k$ . But this given strain is the sum of *genuine mechanical strain* and dimensional increase due to the transformation of RA. The higher part of the given strain value is created by the transformation increase, the lower is determined yield stress (schematically see in Fig. 9). Thus unmonotonous temperature dependence of yield stress is evidence of transformation appearing at relatively low stresses (below conventional yield stress) when only a negligible strain is reached. This means that the controlling agent of the phase transformation of RA is not strain, but stress (see excellent explanation by Tamura [4]). At low temperatures the transformation starts at very low stress due to common effect of tensile stress and decreased temperatures, before a considerable strain is reached. At higher temperatures the stress sufficient for transformation is relatively high. As it can be substantially higher than yield stress, it can be reached only after large strain hardening, i.e. after large strain was obtained.

The maximum decrease of RA content due to deformation to fracture during tensile test was detected at temperature of about  $-108^\circ\text{C}$  (see Fig. 3): the content

decreased from about 35 vol. % of RA to about 20 %. For lower temperatures the initial RA content was lower already due to the cooling of test bars before the tensile test, for higher temperatures the final RA content was higher because at these temperatures no lower RA content could be reached (the temperature dependence of RA content before and after tensile test would be quite analogous to the dependence in Fig. 8 if the scatter of RA content values were not so large). The highest temperature at which the transformation appears due to tensile loading can be estimated at  $M_S^\sigma = (60 \pm 10)^\circ\text{C}$  (see Fig. 3). This temperature characterizing the behaviour at low strains cannot be identified with previously presented temperature  $T_A$  which was determined on the basis of temperature dependence of fracture characteristics connected with the end of deformation process (see Fig. 1).

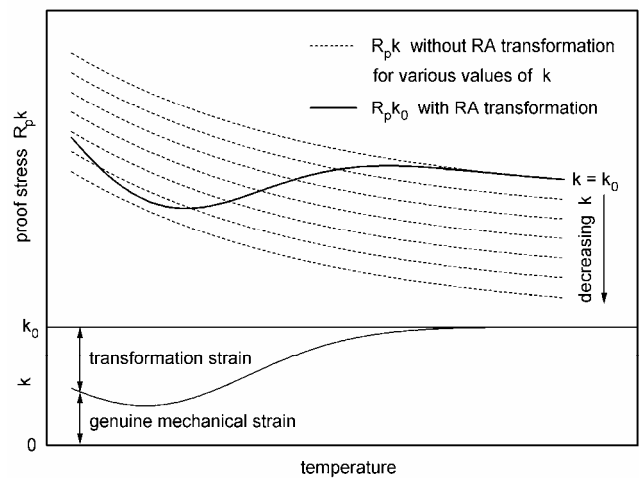


**Fig. 9.** Difference between proof stresses  $R_p k$  for materials without and with phase transformation of RA (schematically)

Studying most of structural materials, static fracture toughness shows higher values than dynamic one at the same temperatures. This effect is explained by the influence of higher loading rates: the increase of strength due to higher rate is predominated by the decrease of deformability of tested material due to the same reason. But the deformability decrease of ADI can be reduced by the dimensional increase due to phase transformation of RA and the extent of this transformation is probably higher for higher loading rates. Then the resulting effect consists in the increase of fracture toughness values. Unfortunately, the changes of RA content in the samples for fracture toughness tests have not been successfully measured, probably because they are concentrated only in the nearest neighbourhood of starting crack.

High and thermally independent values of critical crack dimension are one of substantial advantages of the studied ADI. On the other hand, this effect is based on substantial yield point decrease below room temperature. It can be limiting for the application of ADI for details with high claims for dimensional accuracy, which are used at higher loading.

The most dangerous type of failure of structural material is brittle fracture, which is typical for details loaded at low temperatures. The resistance to the brittle

fracture can be expressed by transition temperatures  $T_D$  and  $T_B$  determining transition region of semi-brittle fractures. Transition temperature of ductility  $T_D$  is the highest temperature at which ductile failure on fracture surface disappears. Usually also a substantial decrease of true fracture stress and deformation characteristics is observed. Transition temperature of brittleness  $T_B$  is the highest temperature at which the failure is created only by wholly brittle fracture. Usually the values of deformation characteristics are very low and the fracture stress is equal to yield stress (this criterion bears some complications for the materials without sharp yield stress including ADI).

Consulting Fig. 1, transition temperature of brittleness lies below the range of testing temperatures. Transition temperature of ductility  $T_D = (-142 \pm 13)^\circ\text{C}$  is very low, fully comparable with the same temperature for nodular cast iron with fully ferritic matrix [5]. Temperature  $T_A = (111 \pm 12)^\circ\text{C}$  at which the increase of deformation characteristics finishes is probably the lowest temperature with fully ductile failure (unfortunately, no microfractographical studies were made for all testing temperatures).

The phase transformation of RA in tested sample can take place all the time between the start of tensile test and the fracture of sample. As the coincidence between the decrease of RA content and yield stress  $R_{p,k}$  is substantially higher than the coincidence between the decrease of RA content and fracture characteristics  $\sigma_{FR}$ ,  $Z$ , and  $A_5$  (from a standpoint of temperature dependence of all the mentioned properties), the conclusion can be made that the majority of transformation takes place in the beginning period of the tensile tests.

Comparing the studied ADI with ADI transformed at lower temperatures of 350 and 300 °C with the structure of transition and lower bainite, respectively, the following division of ADI applicability can be made according to its matrix: lower bainite is the best structural material for static loading [5], transition bainite for impact loading [5] and upper bainite for fatigue loading [7].

## 5. REMARK TO ADI APPLICATIONS

ADI with its excellent mechanical and technological properties belongs among very prospective structural materials. Unfortunately, the peculiarities of its behaviour under mechanical loading mentioned above (anomalous temperature dependence of yield stress, anomalous relation between static and dynamic fracture toughness etc.) are the reason why some less experienced designers are afraid of using it in a larger scale. Good knowledge of ADI behaviour helps to overcome this fear and to make full use of these peculiarities for increasing utility properties of ADI products.

## 6. CONCLUSIONS

On the basis of presented experimental results and their discussion, the following conclusions can be drawn:

1. Obtained unmonotonous temperature dependence of conventional yield stresses of ADI is the consequence of phase transformation of retained austenite. The stress induced martensitic transformation began already before a plastic strain of 0.05 % was reached. The temperatures corresponding to the minima of  $R_{p,k}$  stresses are linear function of logarithm of conventional strain  $\varepsilon_0 = k$ .
2. The distributions of local deformation and the content of retained austenite along the length of sample are rather heterogeneous. It seems that places of maximum rate of transformation are too strengthened to be the places of fracture.
3. Low values of transition temperatures  $T_A$  and  $T_D$  of ADI show that this structural material can be used at low and very low temperatures, if certain deformation due to phase transformation of retained austenite can be accepted.
4. From the practical point of view, the studied ADI is an excellent structural material with high plasticity and toughness, and very good strength.
5. Some peculiarities in ADI mechanical behaviour cannot be a reason why its application should be limited in any way. Experienced designers can use them for increasing utility properties of ADI products.

## Acknowledgments

Financial supports of the Ministry of Defence of the Czech Republic within research project MO0FVT0000404 and of the Grant Agency of the Czech Republic within project 106/03/1265 are gratefully acknowledged.

## REFERENCES

1. Hughes, I. C. H. *Brit. Foundryman* 74 1981: p. 229.
2. Keough, J. R. *Foundry Management and Technology* 123 (11) 1995: p. 27.
3. Dorazil, E. *High Strength Austempered Ductile Cast Iron*. Academia and Horwood, Praha and Chichester, 1991.
4. Tamura, I. *Deformation-induced Martensitic Transformation and Transformation Induced Plasticity in Steels* *Metal Science* 16 (5) 1982: pp. 245–253.
5. Kohout, J. *Deformation and Fracture Behaviour of Unalloyed Nodular Cast Irons* *PhD Thesis* BUT–FME, Brno, 1993 (in Czech).
6. Dorazil, E., Holzmann, M., Crhák, J., Kohout, J. *Influence of Low and Cryogenic Temperature on Deformability and Fracture Behaviour of Austempered Ductile Cast Irons under Static and Impact Stresses* *Giesserei-Praxis* 8/9 1985: pp. 109 – 123.
7. Věchet, S. *Behaviour of Nodular Cast Iron in Conditions of Fatigue Loading* *PhD Thesis* BUT–FME, Brno, 1989 (in Czech).